cAMP diffusion in *Dictyostelium discoideum*: A Green's function method

Daniel S. Calovi, Leonardo G. Brunnet, and Rita M. C. de Almeida
Instituto de Física, Universidade Federal do Rio Grande do Sul, Av. Bento Gonçalves 9500, P.B. 15051, 91501-970 Porto Alegre, RS, Brazil

(Received 14 December 2009; revised manuscript received 14 May 2010; published 15 July 2010; corrected 19 October 2010)

A Green's function method is developed to approach the spatiotemporal equations describing the cAMP production in *Dictyostelium discoideum*, markedly reducing numerical calculations times: cAMP concentrations and gradients are calculated just at the amoeba locations. A single set of parameters is capable of reproducing the different observed behaviors, from cAMP synchronization, spiral waves and reaction-diffusion patterns to streaming and mound formation. After aggregation, the emergence of a circular motion of amoebas, breaking the radial cAMP field symmetry, is observed.

DOI: 10.1103/PhysRevE.82.011909 PACS number(s): 87.10.−e, 87.18.Ed, 87.18.Gh

I. INTRODUCTION

Dictyostelium discoideum (*D. discoideum*) amoebas live in decaying logs as unicellular beings, feeding on bacteria and reproducing by binary fission. Under food shortage they present a different strategy that starts with emission of a chemical signal, cyclic Adenosine 3′,5′ Monophosphate (cAMP). This process begins with a single amoeba inducing others to produce a similar chemical signal in response. They then move toward the growing cAMP concentration and form amoeba streams or spirals, which are oriented to a center where they develop a mound. Subsequently, a tip emerges from this mound which starts to crawl as a multicellular slug. During the mound stage, the amoebas differentiate in two groups: prestalk and prespore. After reaching a more hospitable location, the cells form a stalk supporting the spore which will then disseminate the species throughout the new environment [1]. This interesting behavior of the *D. discoideum* was first reported in 1940 [2].

A comprehensive model of these phenomena must contemplate different stages. A first one, related to the cAMP dynamics by a single cell has been efficiently modeled by Martiel and Golbeter [3], which proposed a set of three evolution equations (MG equations) with parameter values taken from experiments. The second step, cAMP diffusion, necessary to describe cell-cell signaling, was initially dealt with by considering one or several amoebas on each site of a grid [4,5]. The third step is to model the collective behavior, intended to assess the coherent movement of amoebas, capable of forming amoeba streams and in some particular cases, spirals. As the amoeba movement is induced by cAMP gradients, this system presents two interacting dynamics with different time scales. The fast one is related to cAMP signaling [3] and diffusion [4,5]. The slow one has to do with cell movement, which depends on both cAMP gradient and concentration [6]. Since cAMP is produced by cells and their movement is driven by cAMP gradients, these dynamics interact, typically, in a cell size scale. On the other hand, wavelike cAMP fluctuations formed during aggregation may reach the order of centimeters, so, an adequate approach should contemplate the whole time and space extensions. Considering that interactions happen at different time and space scales, we expect that treating them separately will compromise the results.

In fact, models considering single cell dynamics as described by MG equations, but discretizing space with a grid length of the order of cell size, are able to describe cell movement and aggregation. However, they fail to describe the wealth of observed cAMP patterns in the preaggregation stage [7–9]. On the other hand, models simplifying the single cell dynamics but focusing on different aspects of the social cycle of *D. discoideum* also fail to describe aggregation cycle as a whole [10–14]. Although each work has some success in describing a particular feature, the unification of the results is troublesome: taking any of these models, there is not a unique set of parameters capable of describing the whole phenomenon. Reference [15] offers such multifaceted description.

In this work we solve MG equations with diffusion considering all pertinent time and space scales with a unique set of parameters. The results describe the wealth of observed cAMP patterns as well as cell aggregation. The computational cost is greatly reduced by the use of a Green's function to describe diffusion of the cAMP produced by each amoeba. Global cAMP concentration is obtained as the superposition of individual ones. With this approach, the computing time scales with the number of amoebas and is independent of the system size or space dimensions. Each amoeba moves as a boid [16], in a formulation that, besides noise and adhesion [17], is adapted to additionally describe chemotaxis, with a movement efficiency derived from experiments [6]. Our approach aims to show that MG equations (with diffusion) are a minimal model to successfully describe the physically interesting processes involved in the signaling/aggregation stages.

The paper is organized as follows. In Sec. II we show the Green's functions implementation to solve the MG equations [3]. Section III deals with results of the cAMP signaling: synchronization, wave speed, dispersion relation, and reaction-diffusion patterns. Later, on Sec. IV, we introduce movement to the amoebas and present examples of aggregation, streaming and amoeba movement within the mound. In Sec. V we discuss the results and conclude the paper.

II. MODEL EQUATIONS AND METHOD

Martiel and Goldbeter [3] described the cAMP dynamics trough a system of coupled ordinary differential equations.

The parameters of these equations were experimentally acquired. Here we follow the formulation proposed by Nagano [9] to the problem using the MG equations with a diffusion term for the cAMP,

$$\frac{d\gamma(\mathbf{x},t)}{dt} = \frac{k_t}{h}\beta(\mathbf{x},t) - k_e\gamma(\mathbf{x},t) + D\nabla^2\gamma(\mathbf{x},t), \quad (1)$$

$$\beta(\mathbf{x},t) = \sum_{j=1}^{N} \beta_j(t)\exp\left[-\frac{4}{\sigma^2}(\mathbf{x}-\mathbf{x}_j)^2\right], \quad (2)$$

$$\frac{d\beta_j}{dt} = \phi(\rho_j,\gamma_j) - (k_i + k_t)\beta_j, \quad (3)$$

$$\frac{d\rho_j}{dt} = f_2(\gamma_j)(1-\rho_j) - f_1(\gamma_j)\rho_j, \quad (4)$$

where f_1, f_2, ϕ, and Y_j are defined as

$$f_1(\gamma_j) = \frac{k_1 + k_2\gamma_j}{1+\gamma_j}, \quad f_2(\gamma_j) = \frac{k_{-1} + \lambda_1 k_{-2}\gamma_j}{1+\lambda_1\gamma_j},$$

$$\phi(\rho_j,\gamma_j) = \frac{\lambda_2 + Y_j^2}{\lambda_3 + Y_j^2} \times 1800, \quad Y_j = \frac{\rho_j\gamma_j}{1+\gamma_j},$$

this set of equations consists in a three variable system, where σ is the average amoeba diameter. The dynamics of the extracellular cAMP concentration, variable γ in Eq. (1), is regulated, respectively, by terms of source $[\beta(\mathbf{x},t)]$, degradation and diffusion. The coefficient of the source term k_t/h is related to the cAMP amount exported to the extracellular medium, while k_e and D are the degradation and diffusion coefficients, respectively. Variables β_j and ρ_j, are the intracellular concentration and the ratio of active cAMP receptors of the jth amoeba, respectively. These two variables, with dynamics respectively represented by Eqs. (3) and (4), compose the baseline of MG equations, i.e., the dependence on the ratio of active cAMP receptors on the cellular membrane to initiate or maintain internal cAMP production. Equation (2) links the internal cAMP produced $\beta_j(t)$ to a Gaussian spatial distribution of width σ. Most of the parameters used here, are the same biological parameters used by Martiel and Goldbeter, as can be seen in Table I.

Since the only information needed to describe the movement is the cAMP concentration close to the amoebas, we wondered whether numerically solving the diffusion equation for the whole space was indeed the best approach to this problem. If we know the form of a solution for the cAMP diffusion of a single cell, a good approach would be to sum the cAMP contribution from all amoebas. In fact, the single cell solution is given by the Green's function (GF) associated to the problem. The GF indicates how much cAMP produced at time s by the jth amoeba located at $\mathbf{x}_j$ reaches the position $\mathbf{x}$ in space at a time t. Supposing that the cAMP concentration goes to zero far away from each amoeba, we impose null Dirichlet boundary conditions at infinite distance from the origin, we can mathematically define this procedure for a generic point $\mathbf{x}$ in space as

TABLE I. Table of parameter values used in this work. Most values are the same as used in Martiel and Goldbeter paper [3], with the exception of the diffusion constant and the constant h. See text for details.

Parameters	Values used
λ_1	10[a]
λ_2	0.18[a]
λ_3	463.5[a]
k_1	0.036 min^{-1} [a]
k_{-1}	0.36 min^{-1} [a]
k_2	0.666 min^{-1} [a]
k_{-2}	0.00333 min^{-1} [a]
k_i	1.7 min^{-1} [a]
k_t	0.9 min^{-1} [a]
k_e	5.4 min^{-1} [a]
σ	0.01 mm[b]
D	0.024 mm^2/min [b]
h	0.025[c]

[a]Value used in MG's work [3].
[b]Value used in Nagano's work [9].
[c]Value used in this work.

$$\gamma(\mathbf{x},t) = \sum_{j=1}^{N}\int_0^t\int_{-\infty}^{\infty} G(\mathbf{x}-\mathbf{x}_j-\mathbf{y},t-s)f_j(\mathbf{y},s)dsd\mathbf{y}, \quad (5)$$

where $f_j(\mathbf{y},s)$ is the cAMP source, $\mathbf{x}_j$ is the position of the jth particle and $G(\mathbf{x}-\mathbf{x}_j-\mathbf{y},t-s)$ is the Green's function for the diffusion equation with degradation. The solution for the diffusion equation may be found in Ref. [18] and its extension to include degradation can be directly verified applying the corresponding differential operator to the following equation:

$$G(\mathbf{x}_j' - \mathbf{y},t-s) = \frac{1}{[4\pi D(t-s)]^{d/2}} \times\exp\left[-\frac{(\mathbf{x}_j'-\mathbf{y})^2}{4D(t-s)} - k_e(t-s)\right], \quad (6)$$

where d is the dimension of the system and $\mathbf{x}_j' = \mathbf{x} - \mathbf{x}_j$

Nagano's work assumed that the cAMP concentration inside the amoeba is given by a two-dimensional Gaussian as can be seen in Eq. (2). Since the internal cAMP distribution is irrelevant to the external diffusion, we assume that it is homogeneous and take its value directly from the Gaussian center,

$$f_j(\mathbf{y},s) = \begin{cases} \frac{k_t}{2h}\beta_j(s) & \rightarrow \quad \|\mathbf{y}\| \le R_\sigma \\ 0 & \rightarrow \quad \|\mathbf{y}\| > R_\sigma, \end{cases} \quad (7)$$

where R_σ is the radius of the amoeba $(\sigma/2)$. Replacing Eqs. (6) and (7) in Eq. (5) and performing the integration in space, we find

$$\gamma(\mathbf{x},t) = \sum_{j=1}^{N} \int_0^t \frac{c_j(s)}{2^{2d}} \prod_{k=1}^{d} \left[\mathrm{erf}\left(\frac{l_{j,k} + R_\sigma}{\sqrt{4D(t-s)}} \right) - \mathrm{erf}\left(\frac{l_{j,k} - R_\sigma}{\sqrt{4D(t-s)}} \right) \right] \exp^{-k_e(t-s)} \, ds, \quad (8)$$

where $c_j(s) = \frac{k_t}{2h}\beta_j(s)$ is the amount of cAMP that the jth amoeba has created at a time $t-s$, k represents each of the Cartesian coordinates and $l_{j,k}$ is the distance between the jth amoeba and the point where the measure is taken on the coordinate k.

Equation (8) enables us to calculate the cAMP concentration using only an integration and the evaluation of an error function, which are both numerically fast to solve. The downside is that we must keep the cAMP history from each cAMP source. However, this is not expensive to retain since there is an exponential cAMP degradation. This term goes to zero rapidly and only recent data are relevant. Thus, cAMP source history is short enough to make the calculation feasible. Other approaches based on space discretization or spectral methods require grids with resolution much smaller than the amoebas size. The number of grid points being hence, much larger than the number of amoebas. These solutions demand a computational time scaling with the grid size to the power d (system spatial dimension), much longer than our approach that scales with the number of amoebas.

III. CAMP DYNAMICS RESULTS

When an inactive amoeba receives a cAMP stimulus, the receptors bind to cAMP molecules and trigger an internal cycle leading to its own pulse [3]. Once the pulse is emitted the receptors go through a refractory stage with a defined time gap and, until an appropriate fraction of receptors are active again, the amoeba cannot emit a new cAMP pulse. Typically, cAMP pulses happen in a time interval close to ten minutes [19–22].

In this work we assume amoebas with identical biological parameters, so if we start a simulation with all in the same biological initial conditions, they present identical dynamics. In order to describe a set of amoebas with random initial phases, we recorded the biological variables values of a single cell over a whole cycle—we call this *the default cycle*—and randomly distributed these values as initial conditions to the whole set.

It is important to notice that we used the same values as Martiel and Goldbeter for most parameters, the exception being the parameter h, which, in conjunction with parameter k_t, regulates the cAMP source term in MG equations. Nagano used h as a numerical parameter to fit the frequency of pulses to experimental values. Table I presents the full parameter list. With the value used for h, single amoebas cannot signal on their own, but, in a group, they present the experimentally observed oscillation period.

In this part of the work, in order to investigate the cAMP signaling features, the amoebas are kept still and distributed on a regular grid. Spatially close amoebas are known to synchronize their pulses. Such behavior can be seen in Fig. 1 where we present the phase space projection: the intracellular

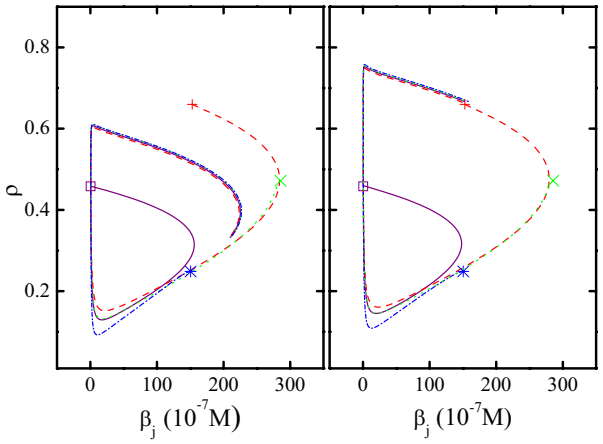

FIG. 1. (Color online) Phase space projection on $\beta_j(10^{-7}$ M) $\times \rho_j$ plane for 4 amoebas (each represented by a different line type) distributed in two squares of lateral sizes of 3σ and 5σ, respectively. Symbols indicate the initial conditions for each trajectory.

cAMP concentration of the jth amoeba, β_j versus the fraction of its active receptors, ρ_j, for 4 amoebas (each represented by a different line type) distributed in two squares with lateral sizes 3σ and 5σ, respectively. Four distinct parts of *the default cycle* were chosen as initial conditions. As can be seen in Fig. 1, synchronization occurs in less than one pulse. As may also be observed in the same figure, the cycle has shrunk in size in the case of the smaller square and the frequency of the pulses has accelerated, both changes are consequence of the higher amoeba density, which saturates cAMP receptors.

In Fig. 1 it can be seen that the dynamics of the amoeba with its initial condition indicated by a square, is forced to shorten its cycle due to the coupling. To better understand the coupling effect among amoebas at long distances we performed numerical experiments with amoebas equally spaced in a rectangular grid (9×80). As we are interested in a two-dimensional system, we have chosen to use 9 columns and, to minimize border effects, only the central amoebas are analyzed. With this setting we performed wave propagation numerical experiments throughout the grid.

The first experiment consists in placing the first row of 9 amoebas in a pulsing state (values from *the default cycle*) and the rest of them in an inactive but susceptible state ($\rho_j = 0.9$ and $\beta_j = 0$). This pulse will induce similar pulses in the neighboring sites producing a cAMP wave. The purpose of this numerical experiment is to determine the effect of the grid density on the cAMP wave propagation speed.

The speed was measured considering the delay it took for the cAMP concentration maximum of a row to reach the next one. Results from the last three rows were omitted due to border effects. In Fig. 2 we present the speed in mm/s for each of the system rows. Simulations were made with amoebas spacings of 8, 24, 27, and 28 (units in σ).

For amoebas spacings lower than 27σ we can also see that the speed, at some time, diverges. This happens due the system density being high enough so that it will eventually present a spontaneous pulse, synchronizing all remaining rows. In systems with amoebas spacings from 28 to 32σ, the

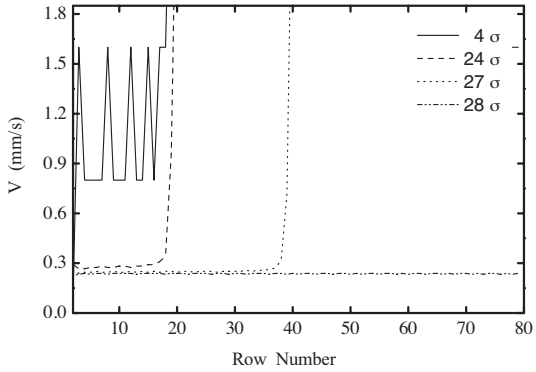

FIG. 2. Wave speed in mm/s versus system rows in a regular grid. The speed was measured considering the delay it takes for cAMP concentration maximum of the previous row to reach the measured one, results from the last rows were omitted due to border effects. Each line represents a simulation with a different amoebas spacings, 8, 24, 27, and 28 all in units of σ.

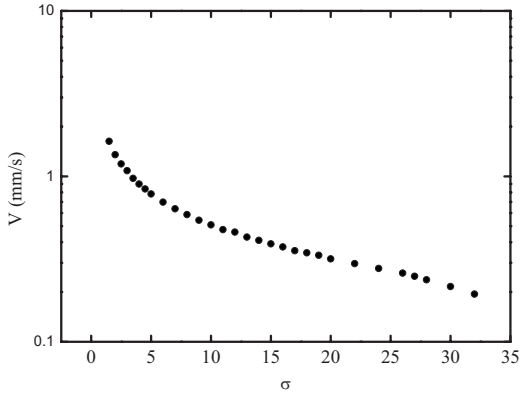

FIG. 3. Average wave speed in mm/s of the previous experiment (as seen in on Fig. 2) which consists in a wave propagating through a regular grid, each simulation with a different spacing. The average was taken before synchronization.

development of the initial pulse into a wave is still observed, but the amoeba density is not high enough to produce spontaneous pulses. That is, it only propagates pulses when imposed as initial condition. For densities lower than that, the pulse degrades before reaching the next row of amoebas and there is no wave front.

It is worth noting that when the system is below the synchronization threshold (i.e., amoebas spacings $<27\sigma$) a wave front imposed to the first row propagates to subsequent rows, farther from the first one. It eventually stabilizes in the middle of the system, generating a wave propagating for both directions.

In Fig. 3 we present the average speed for this experiment (before synchronization), in mm/s, for simulations with amoebas spacings from 1.5 to 32 (units in σ). We can see that speed decreases very fast for low densities probably reflecting the interplay among cAMP diffusion, degradation by phosphodiesterase and the amoeba internal cycle adaptation to the external cAMP concentration. Speeds measured here are within the same order of magnitude of experiments, which vary from 0.26 to 0.5 mm/min [23].

In the second experiment, we studied wave front propagation through the system, using *the default cycle* to distribute the pulses among the rows. Again we used a 9×80 grid and simulated cases with 20, 16, and 10 pulses inserted as initial conditions.

This setting enabled us to analyze the dependence of average cAMP amplitude on the wave number at different densities. For example, for a spacing of 24σ we can simulate wave numbers of values $2\pi/96$, $2\pi/120$, $2\pi/192$ (in $1/\sigma$ units). In Fig. 4 we show the simulation of 10 pulses in a spacing of 24σ, which results in a wave number of $2\pi\sigma^{-1}/192$ We displayed vertically the cAMP concentration of the grid central column, the brightness reflects concentration and the time evolves from left to right.

As our boundary conditions are not periodic, we cannot impose that any pulse reaching one side restarts on the other, so eventually the initial pulses fades away and is replaced by a spontaneous pulse, when the system density allows.

As seen in Fig. 1, depending on the quantity of cAMP in the system, the cycle may shrink, and, under certain conditions, may contract so much that new pulses will be delayed while the cAMP degrades, leaving the system in a quiescent state. Such delay will synchronize most amoebas limiting the maximum density values we may use for a specific quantity of pulses in the system, i.e., wave number. A minimum density value is found when the system is so sparse that the pulses fade away before reaching the next row.

In Fig. 5 we show the average concentration of cAMP amplitude for three sets of pulses at different wave numbers from the previous setting. There is a clear tendency of suppression of the oscillations at high wave numbers. Such behavior is typical of excitable continuous media near an oscillatory instability. This result could be compared to the dispersion relation found for the prototypical complex Ginzburg-Landau [24] equation but the limits imposed by the cAMP dynamics prevent a quantitative comparison.

We can now simulate more complex behavior of cAMP signaling, such as reaction-diffusion patterns. It is known [22] that these patterns are present in early aggregation stages of *D. discoideum*. The model we use allows to simulate such stages without any modification of the default biological parameters. We consider a square grid with equally spaced amoebas. To impose a spatially distributed phase to the system, these amoebas are separated in groups with the

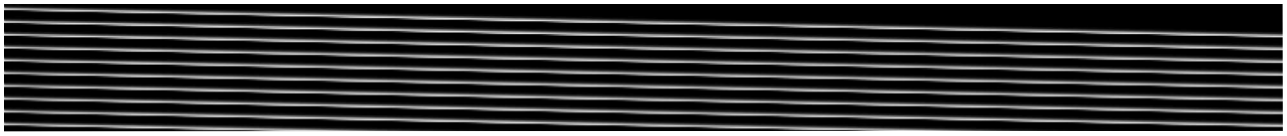

FIG. 4. cAMP concentration of the grid central column is displayed vertically, the brightness reflects concentration and time evolves from left to right. Simulation was made with a spacing of 24σ and with an initial condition of 10 pulses

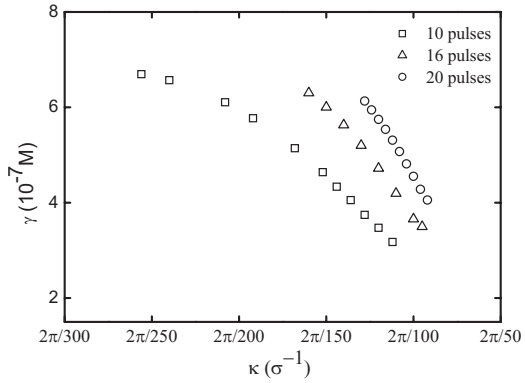

FIG. 5. Average concentration of cAMP amplitude for different wavenumbers (in 10^{-7} $\mathrm{M}\times\sigma^{-1}$ units). Sets of 20, 16, and 10 pulses where chosen as initial conditions on rectangular grids (9×80), i.e., sets of 4, 5, and 8 values sampled on *the default cycle*. For each set of pulses, simulations were made with different spacings, resulting in multiple values for some of the wave numbers.

same initial conditions. Each group contains 9 amoebas, so that the system is composed by $B=N/9$ boxes. A random initial phase of *the default cycle* is attributed to each box.

Figures 6 and 7 show examples of reaction-diffusion patterns for grids of size 18 and 30, with spacings of 13σ and 20σ, respectively. To study the limit where the system goes from circular waves (target) synchronization to spirals or more complex reaction-diffusion patterns, simulations were made with different random initial conditions and densities. We have found that for spacings of 12σ, or lower, the system always converges to a target wave, its size regulates the transient duration. Spacings of 13σ or higher may still evolve to a target wave, but with this density the system may also maintain other structures indefinitely. In fact, spirals and other complex behavior are observed to be more probable for larger and sparser systems in our simulations.

IV. MOVEMENT

To simulate amoeba movement we use a self-propelled particle model with adhesive forces, chemotaxis and noise. Vicsek *et al.* [16] proposed a simple model with self-propelled entities moving in a continuous space with fixed speed and direction dynamically aligned with their neighbors, which have been used as verisimilitude tests in several biologically motivated works [17,25,26].

The work by Vicsek and collaborators in flocking behavior was extended by Gregoire *et al.* [25] to include volume; Belmonte *et al.* [17] extended it further to simulate interactions of different cell types to study the influence of differential adhesion in cellular segregation. In our study Belmonte and collaborators version of the model has been modified to include chemotaxis but with a single adhesive interaction type.

When considering movement, the solution, Eq. (8), of Eq. (1), requires the knowledge of the emission position and intensity history. However, as the cAMP wave propagation is about 25 times faster than the mean amoeba speed [23,27], so the effects of sources displacement may be neglected.

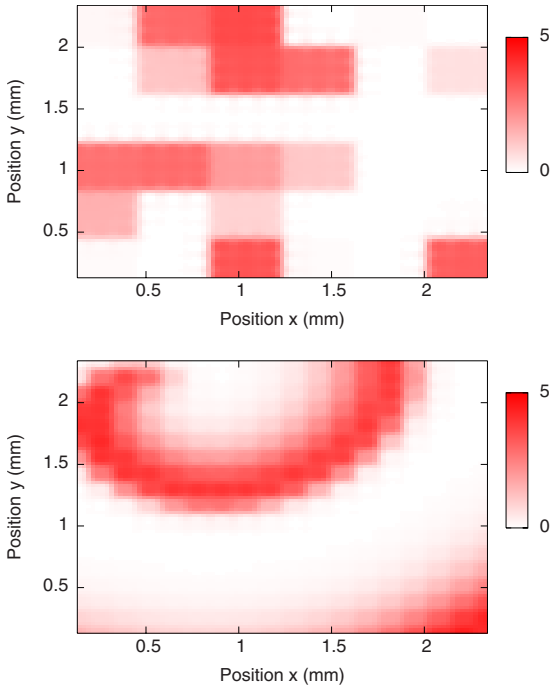

FIG. 6. (Color online) cAMP concentration color map (in 10^{-7} M units) for a square grid (with a spacing of 13σ between amoebas) containing 18×18 amoebas. (a) Initial condition with 36 states randomly obtained from *the default cycle*. These states were distributed among an equal number of boxes, each containing 9 amoebas. (b) Evolution to a spiral of that initial condition after 110 min of simulation. See Ref. [38] for a movie on the pattern evolution.

In our simulations amoebas are supposed to a have fixed speed, $v_0=2$ μm/min, a value taken from previous experiments [27]. The kinetic state of the ith amoeba at a time t is described by its location, $\mathbf{x}_i^t$, and by the direction of its velocity, $\boldsymbol{\theta}_i^t$ (in two dimensions). This orientation angle is obtained as in Ref. [17], but with a chemotaxis term added,

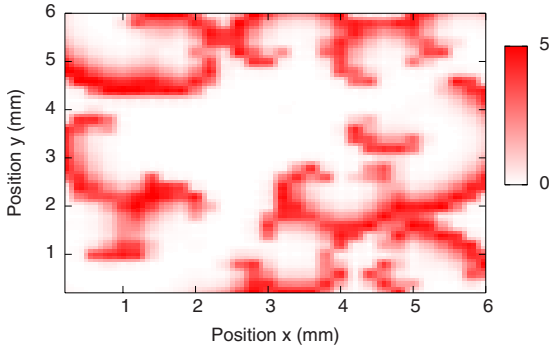

FIG. 7. (Color online) cAMP concentration color map (in 10^{-7} M units) for a square grid (with a spacing of 20σ between amoebas) containing 30×30 amoebas. The image shows the evolution of the 100 states randomly obtained from *the default cycle*, distributed among an equal number of boxes, each containing 9 amoebas. After 20 min of simulation, we can observe a complex reaction-diffusion pattern. See Ref. [38] for a movie on the pattern evolution.

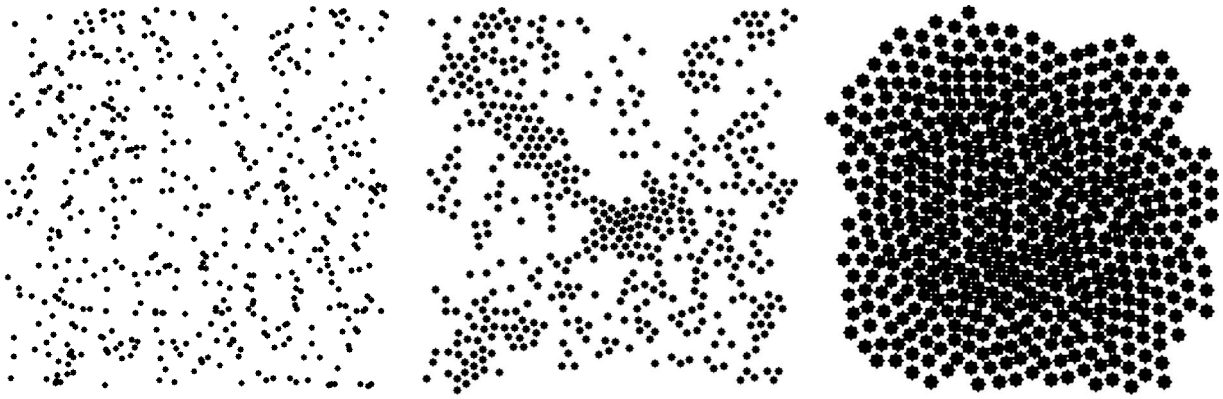

FIG. 8. Aggregation states of 500 amoebas randomly distributed on a square of side 0.45 mm. The initial state for each amoeba was randomly chosen from *the default cycle*. The image shows three different simulation states: (a) $T=0$, (b) $T=5$ min, (c) $T=15$ min. See Ref. [38] for a movie on amoebas aggregation.

$$\boldsymbol{\theta}_i^{+1} = \arg\left[\sum_{\substack{j=1 \\ j\neq i}}^{n} \nu f_{ij}^t \mathbf{e}_{ij}^t + \eta \mathbf{u}_i^t + \epsilon g_i(\gamma^t)\frac{\boldsymbol{\nabla}\gamma^t}{|\boldsymbol{\nabla}\gamma^t|}\right]. \tag{9}$$

The first term is responsible for the interaction between amoebas; it is a radial force, f_{ij}^t, that is exerted by particle j on the particle i along the direction $\mathbf{e}_{ij}^t$ that goes from particle j to the particle i; parameter ν controls its weight. Parameter η controls the intensity of the noise which is an unitary vector with random uniformly distributed orientation, $\mathbf{u}_i^t$. The last term represents the chemotaxis, described here as an unitary vector pointing in the cAMP concentration direction multiplied by a density dependent scalar function $g_i(\gamma^t)$ and relative weight controlled by parameter ϵ. Experiments [6] show that the movement efficiency toward the cAMP gradient is highly influenced by the cAMP concentration. We linearly interpolated the data points extracted from Fig. 5 of Ref. [6] to construct the function $g_i(\gamma^t)$ in the above equation.

The radial force used contains a hard core repulsion for interactions within a radius d_c and a linear term for interactions in the interval $d_c < r < d_0$, the latter being defined using the equilibrium distance d_e,

$$f_{ij} = \begin{cases} \infty & \text{if } r_{ij} < d_c, \\ 1 - \dfrac{r_{ij}}{d_e} & \text{if } d_c < r_{ij} < d_0, \\ 0 & \text{if } r_{ij} > d_0, \end{cases} \tag{10}$$

where $d_c = 0.75\sigma$, $d_0 = 1.125\sigma$, and $d_e = \sigma$.

It can be inferred from Eq. (9) that when amoebas are close to each other, the values of η, ν, and ϵ must be adequately chosen. Preliminary simulations have shown that, at the moment of a pulse, chemotaxis may overcome the radial force. For the parameter settings for which this happens, the aggregate size oscillates along with the cAMP pulses. As far as we know, this is not seen in experiments. So, the parameters controlling the amoebas movement should be chosen to avoid this behavior.

In Figs. 8 and 9 we show a group of 500 amoebas randomly distributed on squares of sides 0.45 and 1 mm, respectively. The initial conditions for each amoeba were randomly sampled from *the default cycle*. Each image presents snapshots at different system evolution stages. Figure 9(b) shows indications of streaming after 5 min of evolution. After 30 min [Fig. 9(c)] we have five different aggregates, contrasting with Fig. 8(c) which presents a single aggregate. Both simu-

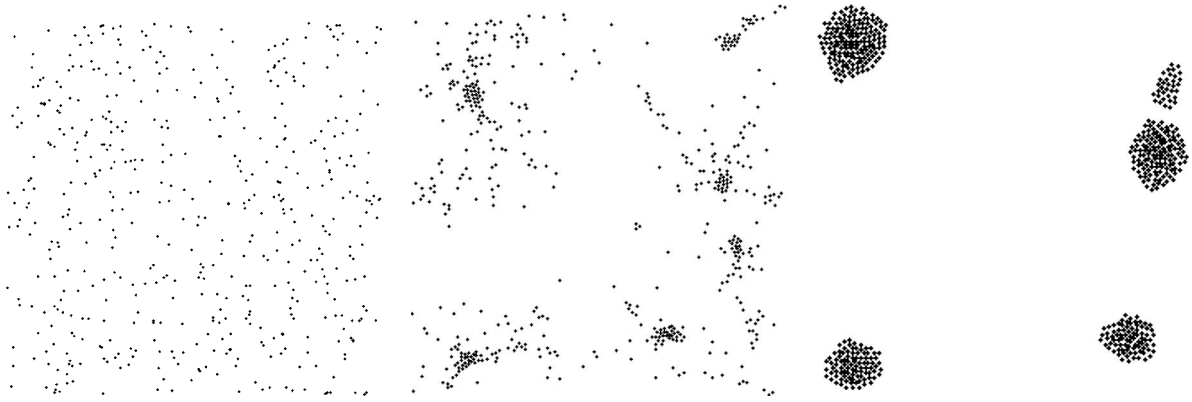

FIG. 9. Aggregation states of 500 amoebas randomly distributed on a square of side 0.45 mm. The initial state for each amoeba was randomly chosen from *the default cycle*. Image shows three different states of the simulation: (a) $T=0$, (b) $T=5$ min, (c) $T=25$ min. See Ref. [38] for a movie on amoebas aggregation.

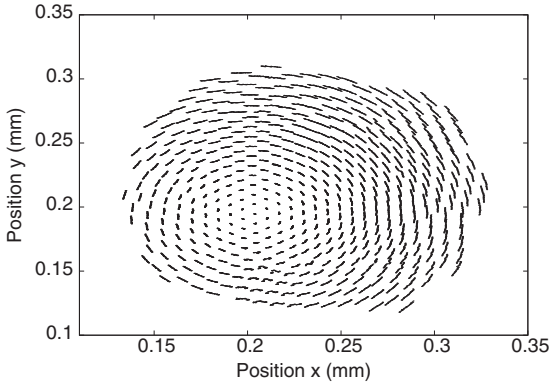

FIG. 10. Amoebas trajectories from Fig. 8 over a 40 min (50 min$<t<$90 min) simulation window, where a collective rotational behavior can be seen.

lations were performed with the following movement parameters: ν=8, ϵ=4, and η=1.

To obtain finer details about the internal structure of the aggregate presented in Fig. 8(c), we studied the effect of the movement parameters on the aggregate asymptotic behavior. Fixing the noise value to η=1, the parameters, ν and ϵ, remain free. There are two clear limits where parameters ϵ or ν dominate the system: (i) in the case where chemotaxis is more relevant, the system, once aggregated, contracts up to the core limit, reacting like rigid disks under compression; (ii) if radial force dominates, each amoeba moves around a central equilibrium point, as particles vibrating in a spring lattice.

In the intermediary parameter range, we find an interesting collective internal movement. This behavior is shown on Fig. 10 which represents the amoebas trajectories over a 40 min simulation window. It shows a collective circular motion that reflects internal streaming and suggests that the helicoidal order of amoebas streams found in the slug may emerge in a similar way.

V. DISCUSSION AND CONCLUSIONS

We present here a model based on the Martiel and Goldbeter equations with a diffusion term solved using Green's functions, which determine cAMP concentration and gradient directly on each amoeba, avoiding cAMP calculation at all points in space. As a consequence, simulation times scale with the number of amoebas and not with system size or space dimension. This is a great advantage when comparing to simulations with discrete space, since in the latter the system size or space dimension will impact on the numerical cost to solve it.

Several *D. discoideum* properties, from initial aggregation stages up to mound formation, were reproduced. The values of almost all cAMP signaling parameters are taken from Martiel and Goldbeter work [3] which were based on experiments, with exception of the diffusion coefficient value, taken from Naganos paper [9], and parameter h, that controls the intensity of cAMP production by the amoebas, used as a free parameter to tune the system.

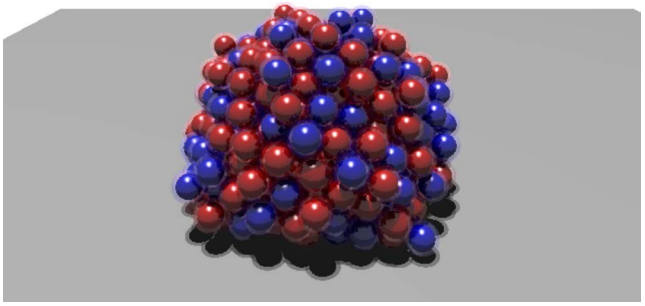

FIG. 11. (Color online) Aggregate formed by 500 amoebas which were initially distributed in a 45 mm square. Different shades are used to make visualization easier.

To determine the basic properties of cAMP diffusion, we considered a set of simulations using amoebas fixed in space. Depending on amoebas density, three different regimes were found: no wave front propagation, cAMP wave propagation under stimulus, and synchronization. Moreover the measured speeds were compatible with experimental values [23]. Also, an equally spaced group of fixed amoebas was set, sequentially, to different phases of their *default cycle* to study the dispersion relation between wave number and cAMP oscillation amplitude. We find the same qualitative behavior as in solutions of complex Ginzburg-Landau equation [24] with an amplitude decay at large wave numbers. A quantitative fit was not possible, since it would require data sets larger than the limits imposed by amoebas density.

Reaction-diffusion patterns naturally appear in the model, although at a lower density than the experimentally observed [28]. Here, spacings smaller than 12σ always converge to a target wave pattern. The reasons for these discrepancies may be many. We point out that while this model uses fixed parameters, certain biological properties may adapt to different stimuli on experiments. Also, the role of phosphodiesterase may be underestimated [7]. In fact, larger values of the degradation parameter k_e are expected to yield reaction diffusion patterns at higher densities.

Amoeba movement was simulated using a boids model [16,17,25]. The amoebas aggregated as expected, showing stream formation in the early stages. In Fig. 9 we have seen that depending on the density, the amoebas might form more than a single aggregate. The formation of multiple aggregates at lower densities was expected due to the nature of the MG's equations. As seen in Fig. 1, when the system density becomes extremely high (aggregation), the oscillatory cycle shrinks to a point in the phase space projection $\beta_j \times \rho_j$. Despite an average cAMP concentration of 2×10^{-7} M on these aggregates, we can see if Fig. 5 that, at low densities, pulses do reach higher amplitudes, and in doing so, they attract much farther amoebas.

Also, as discussed in the beginning of Sec. II, using the free parameter h, we may control the necessary cAMP quantity produced by the amoebas in order to keep the system oscillating and attracting distant amoebas, until a given amount of amoebas reach the aggregate. Further investigation is required to establish whether there is a value for which this oscillation period is similar to experiments and a greater number of amoebas aggregates before the cAMP pro-

duction reaches a constant plateau, or whether it would be necessary to implement an adaptable parameter h so that the features of *D. discoideum* could be more accurately simulated.

Circular and helicoidal motion are observed at different stages of the *D. discoideum* social cycle [29,30]. Interestingly, after aggregation is complete in our simulations, internal circular motion emerges (Fig. 10). This behavior has been found in previous *D. discoideum* simulations [31] and also in models of self-propelled elements where some kind of confinement is imposed by considering either repulsive walls [32] or forces acting toward the cluster gravitational center [33]. Here confinement is a consequence of the radial cAMP field pattern installed after aggregation and, consequently, the circular motion solution implies a spontaneous symmetry breaking. This is an alternative to the current hypothesis of a circular/helicoidal cAMP field [34].

This numerical solution may be readily implemented in three dimensions. Preliminary tests produced the three dimensional mound with 500 amoebas shown in Fig. 11. At the beginning of this simulation, the amoebas were randomly placed on a square plane with 45 mm side.

To conclude, alternative models could have been considered to describe cAMP production. For example, Refs. [35,36] considered a different, simpler biochemical approach but the parameters used are not experimentally obtained. In Ref. [37], on the other hand, a more detailed description of cAMP production is proposed. However, for the *D. discoideum* life stages treated here, this increased complexity is not necessary. Our approach has shown that MG equations (with diffusion) are an excellent minimal model to describe the whole processes involved in the signaling and aggregation stages of *D. discoideum*.

ACKNOWLEDGMENT

The authors thank the Brazilian agencies CNPq, CAPES, and FAPERGS for the financial support.

[1] *Developmental Biology*, edited by S. F. Gilbert (Sinauer Associates, Inc., Sunderland, MA, 1997).
[2] J. R. Raper, J. Elisha Mitchell Sci. Soc. **56**, 241 (1940).
[3] J.-L. Martiel and A. Goldbeter, Biophys. J. **52**, 807 (1987).
[4] J. J. Tyson and J. D. Murray, Development **106**, 421 (1989).
[5] J. J. Tyson, K. A. Alexander, V. S. Manoranjan, and J. D. Murray, Physica D **34**, 193 (1989).
[6] P. R. Fisher, R. Merkl, and G. Gerisch, J. Cell Biol. **108**, 973 (1989).
[7] T. Bretschneider, B. Vasiev, and C. J. Weijer, J. Theor. Biol. **189**, 41 (1997).
[8] T. Bretschneider, B. Vasiev, and C. J. Weijer, J. Theor. Biol. **199**, 125 (1999).
[9] S. Nagano, Phys. Rev. Lett. **80**, 4826 (1998).
[10] H. Levine and W. Reynolds, Phys. Rev. Lett. **66**, 2400 (1991).
[11] D. A. Kessler and H. Levine, Phys. Rev. E **48**, 4801 (1993).
[12] O. O. Vasieva, B. N. Vasiev, V. A. Karpov, and A. N. Zaikin, J. Theor. Biol. **171**, 361 (1994).
[13] B. N. Vasiev, P. Hogeweg, and A. V. Panfilov, Phys. Rev. Lett. **73**, 3173 (1994).
[14] N. J. Savill and P. Hogeweg, J. Theor. Biol. **184**, 229 (1997).
[15] A. F. M. Marée, A. V. Panfilov, and P. Hogeweg, J. Theor. Biol. **199**, 297 (1999).
[16] T. Vicsek, A. Czirók, E. Ben-Jacob, I. Cohen, and O. Shochet, Phys. Rev. Lett. **75**, 1226 (1995).
[17] J. M. Belmonte, G. L. Thomas, L. G. Brunnet, R. M. C. de Almeida, and H. Chaté, Phys. Rev. Lett. **100**, 248702 (2008).
[18] E. Butkov, *Mathematical Physics* (Addison-Wesley, Reading, MA, 1968).
[19] G. Gerisch, D. Malchow, W. Roos, and U. Wick, J. Exp. Biol. **81**, 33 (1979).
[20] A. J. Durston, Dev. Biol. **37**, 225 (1974).
[21] F. Siegert and C. J. Weijer, Physica D **49**, 224 (1991).
[22] F. Alcantra and M. Monk, J. Gen. Microbiol. **85**, 321 (1974).
[23] F. Siegert and C. Weijer, J. Cell. Sci. **93**, 325 (1989).
[24] S. Popp, O. Stiller, I. Aranson, A. Weber, and L. Kramer, Phys. Rev. Lett. **70**, 3880 (1993).
[25] G. Grégoire and H. Chaté, Phys. Rev. Lett. **92**, 025702 (2004).
[26] S. Hubbard, P. Babak, S. T. Sigurdsson, and K. G. Magnusson, Ecol. Modell. **174**, 359 (2004).
[27] T. Hofer, J. A. Sherratt, and P. K. Maini, Proc. R. Soc. London, Ser. B **259**, 249 (1995).
[28] K. J. Lee, E. C. Cox, and R. E. Goldstein, Phys. Rev. Lett. **76**, 1174 (1996).
[29] F. Siegert and C. J. Weijer, Proc. Natl. Acad. Sci. U.S.A. **89**, 6433 (1992).
[30] F. Siegert and C. J. Weijer, Curr. Biol. **5**, 937 (1995).
[31] W.-J. Rappel, A. Nicol, A. Sarkissian, H. Levine, and W. F. Loomis, Phys. Rev. Lett. **83**, 1247 (1999).
[32] B. Szabó, G. J. Szölösi, B. Gönci, Z. Jurányi, D. Selmeczi, and T. Vicsek, Phys. Rev. E **74**, 061908 (2006).
[33] N. Shimoyama, K. Sugawara, T. Mizuguchi, Y. Hayakawa, and M. Sano, Phys. Rev. Lett. **76**, 3870 (1996).
[34] J. Rietdorf, F. Siegert, S. Dharmavardhane, R. A. Firtel, and C. J. Weijer, Dev. Biol. **181**, 79 (1997).
[35] J. C. Dallon and H. G. Othmer, Philos. Trans. R. Soc. London, Ser. B **352**, 391 (1997).
[36] E. Palsson and H. G. Othmer, Proc. Natl. Acad. Sci. U.S.A. **97**, 10448 (2000).
[37] M. T. Laub and W. F. Loomis, Mol. Biol. Cell **9**, 3521 (1998).
[38] See supplementary material at http://link.aps.org/supplemental/10.1103/PhysRevE.82.011909 for a movie on the pattern evolution of amoebas as in Figs. 6–9.